Energy dependence of directed flow in Au + Au collisions from a multiphase transport model

J. Y. Chen,[1,*] J. X. Zuo,[2,†] X. Z. Cai,[3] F. Liu,[1] Y. G. Ma,[3] and A. H. Tang[4]

[1]*Institution of Particle Physics, Huazhong Normal University (CCNU), Wuhan 430079, People's Republic of China and The Key Laboratory of Quark and Lepton Physics (Huazhong Normal University), Ministry of Education, Wuhan 430079, People's Republic of China*

[2]*Institute of High Energy Physics, CAS, Beijing 100049, People's Republic of China*

[3]*Shanghai Institute of Applied Physics, CAS, Shanghai 201800, People's Republic of China*

[4]*Physics Department, Brookhaven National Laboratory, Upton, New York 11973, USA*

(Received 10 October 2009; published 8 January 2010)

The directed flow of charged hadron and identified particles has been studied in the framework of a multiphase transport (AMPT) model for ^{197}Au + ^{197}Au collisions at $\sqrt{s_{NN}}$ = 200, 130, 62.4, 39, 17.2, and 9.2 GeV. The rapidity, centrality, and energy dependence of directed flow for charged particles over a wide rapidity range are presented. The AMPT model gives the correct $v_1(y)$ slope, as well as its trend as a function of energy, while it underestimates the magnitude. Within the AMPT model, the proton v_1 slope is found to change its sign when the energy increases to 130 GeV—a feature that is consistent with "anti-flow." Hadronic rescattering is found to have little effect on v_1 at top energies currently available at the BNL Relativistic Heavy Ion Collider (RHIC). These studies can help us to understand the collective dynamics early on in relativistic heavy-ion collisions, and they can also be served as references for the RHIC Beam Energy Scan Program.

DOI: 10.1103/PhysRevC.81.014904 PACS number(s): 25.75.Ld, 24.10.−i, 25.75.Nq, 25.75.Dw

I. INTRODUCTION

Anisotropic flow is one of the key observables in characterizing properties of the dense and hot medium created in relativistic heavy-ion collisions [1]. It is quantified by Fourier coefficients when expanding particle's azimuthal distribution with respect to the reaction plane [2]:

$$E\frac{d^3N}{d^3p} = \frac{1}{2\pi}\frac{d^2N}{p_T dp_T dy}\left(1 + \sum_{n=1}^{\infty} 2v_n \cos n\phi\right), \qquad (1)$$

where ϕ denotes the angle between the particle's azimuthal angle in momentum space and the reaction plane angle. The sine terms in Fourier expansions vanish due to the reflection symmetry with respect to the reaction plane. The various coefficients in this expansion can be defined as

$$v_n = \langle \cos n\phi \rangle. \qquad (2)$$

The first and second coefficients are named as directed flow (v_1) and elliptic flow (v_2), respectively, and they play important roles in describing the collective expansion in azimuthal space. Elliptic flow is produced by the conversion of the initial coordinate-space anisotropy into momentum-space anisotropy, due to the developed large in-plane pressure gradient. Elliptic flow depends strongly on the rescattering of the system constituents; thus it is sensitive to the degree of thermalization [3] of the system early on. Directed flow, which is the focus of this study, describes the "side splash" of particles away from midrapidity [4], and it probes the dynamics of the system in the longitudinal direction. Because directed flow is generated very early, it brings information from the foremost early collective motion of the system. The shapes of directed flow, in particular those for identified particles, are of special interest because they are sensitive to the equation of state (EOS) and may carry a phase transition signal [5].

The study of energy dependence of directed flow has implications in many aspects. First, because directed flow has a unique, pre-equilibrium origin, it is expected to behave differently than other soft observables that show an "entropy-driven" multiplicity scaling [6]. It has been shown by the solenoidal tracker at the BNL Relativistic Heavy Ion Collider (STAR) detector [7] that at top energies currently available at the BNL Relativistic Heavy Ion Collider (RHIC) directed flow is independent of system size, whereas it has an energy dependence. For a comprehensive study of the subject, it is necessary to extend the study of the energy dependence of directed flow in a wider energy range. Second, experiments at RHIC (PHENIX and STAR) have planned to look for the existence of the QCD phase boundary and the possible critical point by colliding heavy ions at various incident beam energies [8–10]. A nonmonotonic dependence of variables on $\sqrt{s_{NN}}$ and an increase in event-by-event fluctuations should become apparent near the critical point [8]. Directed flow is generated during the nuclear passage time ($2R/\gamma \sim 0.1$ fm/c) and it probes the onset of bulk collective dynamics in the earlier stage of the collision. As a suggested signature of a first-order phase transition [5], directed flow is sensitive to the creation of the critical point and it plays an important role in the proposed beam energy scan program.

In this article, directed flow from the AMPT model for six energies is presented. They are 9.2, 17.3, 39, 62.4, 130, and 200 GeV. The comparisons with the measurements from STAR and PHOBOS are made at top energies. The particle type dependence over a wide rapidity range is discussed. This study will deepen our understanding about the energy dependence of directed flow, and it can also serve as a valuable reference for the RHIC Beam Energy Scan Program.

*chenjy@iopp.ccnu.edu.cn
†zuojx@ihep.ac.cn

II. THE AMPT MODEL

The AMPT model consists of four main components [11]: initial conditions, partonic interactions, conversion from partonic matter to hadronic matter, and hadronic interactions. The initial conditions, which include the spatial and momentum distributions of the mini-jet partons and soft string excitations, are obtained from the HIJING model [12]. The scatterings among partons are modeled by Zhang's parton cascade (ZPC) [13], which includes two-body scatterings with cross sections from pQCD with screening masses. In the default AMPT model [14], partons are recombined with their parent strings when they stop interacting, and the resulting strings fragment into hadrons according to the Lund string fragmentation model [15]. In the AMPT model with string melting [16], quark coalescence is used instead to combine partons into hadrons. The dynamics of the subsequent hadronic matter is described by the ART (a relativistic transport) model [17] with modifications and extensions. As suggested in Ref. [18], the parton cross section is chosen as 3 mb in our analysis. All the errors presented here are statistical only.

III. ANALYSIS AND RESULTS

In Fig. 1, the directed flow of charged particles from the AMPT model is shown as a function of rapidity for collision energies of 200, 130, 62.4, 39, 17.2, and 9.2 GeV. The centrality is divided into three bins, namely, 0%–30%, 30%–60%, and 60%–80%, based on the impact parameter (b) distribution. Calculations with the string melting scenario are used for high energies (200, 130, 62.4, and 39 GeV) whereas for low energies (17.2 and 9.2 GeV) calculations are performed with the default scenario. The reason for such a choice is because it is argued

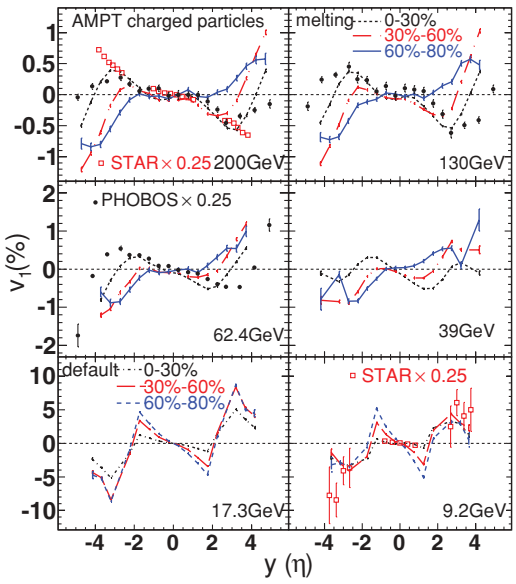

FIG. 1. (Color online) Rapidity dependence of v_1 for charged particles in the AMPT model compared with STAR and PHOBOS data (plotted as a function of η) in Au + Au collisions at $\sqrt{s_{NN}} =$ 200 GeV. The dashed lines show AMPT results from different centralities: 0%–30% (black), 30%–60% (red), 60%–80% (blue).

[18–20] that the string melting should be used to explain flow around midrapidity at top RHIC energies, and the default setting describes data at 9.2 GeV the best. The energy density in the collisions at the top energies available at the RHIC is much higher than the critical density for the QCD phase transition. More discussion on different AMPT configurations can be found later in this article. All results are obtained by integrating over transverse momentum (p_T) up to 4.0 GeV/c. Experimental results from STAR [7,21] and PHOBOS [22] are also shown for comparison. The charged hadron v_1 measured by the PHOBOS experiment is for 0%–40% central collisions, and the results measured by the STAR experiment are for centrality 30%–60% at 200 GeV and centrality 0–60% at 9.2 GeV. In general, the AMPT model gives larger v_1 at low energies than at high energies; the same trend has been seen in experimental data. At top RHIC energies, the AMPT model underestimated v_1, due to the turnoff of mean-field potentials in ART when implemented in the AMPT model to describe the hadronic scattering [11]. However, in the rapidity range of [−2.0,2.0], the shape of v_1 between the AMPT calculations and experimental data are in good agreement—this can be seen by scaling experimental results with a factor of 0.25.

The particle type dependence of directed flow is shown in Fig. 2. The different sign of v_1 between pions and protons at low energies can be understood as nucleon shadowing and baryon stopping [23,24]. In general the magnitude of the v_1 slope at midrapidity decreases with increasing energy. This effect is most profound for protons, for which the slope keeps decreasing, and when the energy is high enough it changes its sign and protons begin to flow together with pions. This is consistent with the "anti-flow" scenario [25], in which the "bounce-off" motion and transverse expansion of nucleons compete with each other around midrapidity, and when the transverse expansion is strong enough (e.g., at top RHIC energies), it overcomes the "bounce-off" motion and causes protons to change their sign of directed flow.

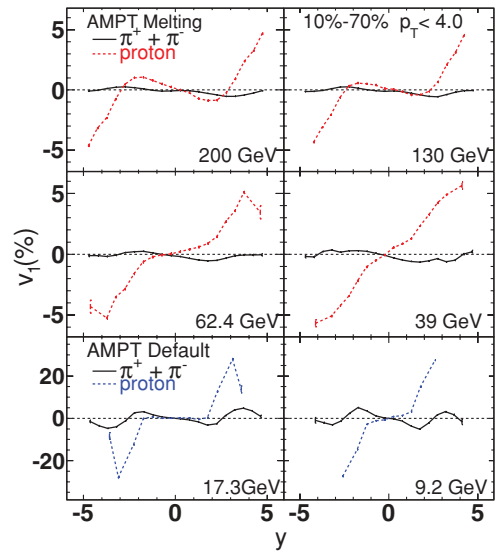

FIG. 2. (Color online) Proton (solid lines) and pion (dashed lines) $v_1(y)$ from AMPT at centrality 10%–70%.

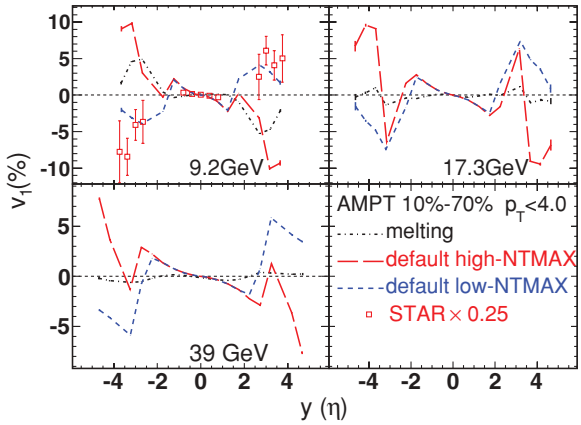

FIG. 3. (Color online) Charged particles $v_1(y)$ from centrality 10%–70% for 9.2 GeV (upper-left panel), 17.3 GeV (upper-right panel), and 39 GeV (lower-left panel). The dashed lines show three AMPT versions: string melting scenario (black), default scenario with high-NTMAX (red), and low-NTMAX (blue). Experimental data points from STAR are plotted as a function of η.

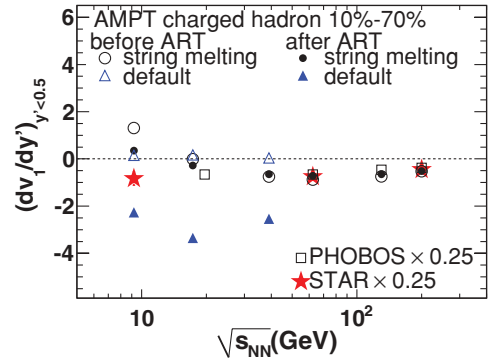

FIG. 4. (Color online) Charged hadrons' slope dv_1/dy' around midrapidity ($|y'| < 0.5$) as a function of incident energy. The data are taken from STAR (stars) and PHOBOS (squares) and scaled by a factor 0.25. The AMPT calculations with string melting before ART are depicted with open circles and after hadron cascade they are depicted with solid circles. The open triangles depict the default AMPT calculations before ART and the solid triangles depict the calculations after hadron cascade.

To illustrate the effect on v_1 due to different configurations in the AMPT model, in Fig. 3 we present the directed flow of charged hadrons in low-energy collisions obtained from AMPT calculations with the string melting scenario and the default scenario. A similar study for higher energies can be found in Ref. [18]. The calculation with string melting yields the smallest v_1 slope around midrapidity and is close to experimental data. Two different default scenarios are also studied: one is calculated with NTMAX = 2500 (high NTMAX) and the other with NTMAX = 150 (low NTMAX). NTMAX stands for the number of time steps for the hadron cascade (see detail in Ref. [11]). A large NTMAX means a thoroughly developed hadron cascade, as 0.2 fm/c *NTMAX is the termination time in the center of mass frame of the hadron cascade in the AMPT model. The comparison, for low energies, of v_1 calculated between low NTMAX and high NTMAX indicates that v_1 can change its sign at large rapidity if the time for the hadronic cascade is long enough. In the default AMPT calculations, the NTMAX must be much larger than 150 to describe v_1 at large rapidity. The disagreement between the experimental data and the calculation made with high NTMAX is mostly due to the lack of mean field in the hadron cascade in the AMPT model, which has a considerable effect at low energies when the nuclei passage time is not negligible (compared to that at high energies). The AMPT calculation with high NTMAX at high energy is presented in Ref. [26]. In this article, we address the comparison around midrapidity only, and results presented in this article are made with low NTMAX unless otherwise specified.

The energy dependence of charged particle directed flow, calculated with the AMPT model, is shown in Fig. 4. Experimental data are also shown for comparison. The centrality for which the calculation is performed is 10%–70%. The centrality for the PHOBOS data from different energies is 0%–40% whereas the centrality selections for the STAR data are 0%–60% for 9.2 GeV, 10%–70% for 62.4 GeV, and 30%–60% for 200 GeV. To obtain the integrated v_1, one needs to fold in the spectra at different energies, which brings in an additional layer of systematics. Thus instead, we present the slope of $v_1(y)$ around midrapidity ($|y'| < 0.5$) extracted from the normalized ($y' = y/y_{\text{beam}}$) rapidity distribution, where y_{beam} is the beam rapidity. For the energy range in which string melting is used (39 GeV and above), all the AMPT calculations underestimate the experimental data; however, they predict the right trend of the energy dependence. For the low energies at 9.2 GeV, calculations with string melting did a poor job, the calculation with the default AMPT improves the result in the right direction yet is still not be able to explain the data. The hadron rescattering effect on directed flow v_1 can be seen by switching off the hadron cascade in the AMPT calculation. By comparing the difference between the result with hadron cascade (open symbols) and without (solid symbols), it is found that the hadronic cascade has a significant effect for low-energy results but little effect for high energies. In other words, when the energy is high enough, the hadron rescattering becomes less important because of the presence of strong collective motion built up beforehand.

IV. SUMMARY AND CONCLUSIONS

In this article, v_1 values calculated from the AMPT model for different energies are discussed. It is found that the AMPT model gives the right shape of v_1 versus y while underestimating the magnitude, possibly due to the lack of mean field in its hadron cascade. In AMPT, the proton v_1 slope changes its sign when the energy increases to 130 GeV and begins to have the same sign as that of pions, as expected in the "anti-flow" scenario. The effects on v_1 due to string melting, low NTMAX, and high NTMAX are illustrated. The energy dependence of the v_1 slope at midrapidity is compared to experimental data, and the AMPT model can describe the trend of energy dependence while missing the magnitude by a fraction of 75%. Hadronic rescattering is found to be less

important at high energies as the strong collective motion comes to be the dominant dynamics.

ACKNOWLEDGMENTS

The authors greatly thank Zi-Wei Lin and Zhangbu Xu for useful discussions and kindly providing comments on the manuscript. The authors appreciate Matthew Lamont's help with the English. This work was supported in part by the National Natural Science Foundation of China under Grants 10775058 and 10610285, the MOE of China under Grant IRT0624, the MOST of China under Grant 2008CB817707, and the Knowledge Innovation Project of the Chinese Academy of Sciences under Grants KJCX2-YW-A14 and KJCX3-SYW-N2.

[1] For a recent review, see: S. A. Voloshin, A. M. Poskanzer, and R. Snellings, arXiv:0809.2949 [nucl-ex].
[2] A. M. Poskanzer and S. A. Voloshin, Phys. Rev. C **58**, 1671 (1998).
[3] P. F. Kolb, J. Sollfrank, and U. Heinz, Phys. Rev. C **62**, 054909 (2000).
[4] H. Sorge, Phys. Rev. Lett. **78**, 2309 (1997).
[5] H. Stocker, Nucl. Phys. **A750**, 121 (2005).
[6] A. H. Tang, J. Phys. G **34**, S277 (2007); H. Song and U. Heinz, Phys. Rev. C **78**, 024902 (2008); J. Chen (STAR Collaboration), J. Phys. G **35**, 044072 (2008).
[7] B. I. Abelev *et al.* (STAR Collaboration), Phys. Rev. Lett. **101**, 252301 (2008).
[8] P. Sorensen (STAR Collaboration), arXiv:nucl-ex/0701028v1.
[9] G. Odyniec (STAR Collaboration), J. Phys. G **35**, 104164 (2008).
[10] T. Sakaguchi (PHENIX Collaboration), arXiv:0908.3655 [nucl-ex].
[11] Z. W. Lin, C. M. Ko, B. A. Li, B. Zhang, and S. Pal, Phys. Rev. C **72**, 064901 (2005).
[12] X. N. Wang and M. Gyulassy, Phys. Rev. D **45**, 844 (1992); M. Gyulassy and X. N. Wang, Comput. Phys. Commun. **83**, 307 (1994).
[13] B. Zhang, Comput. Phys. Commun. **109**, 193 (1998).
[14] Z. W. Lin and C. M. Ko, Phys. Rev. C **68**, 054904 (2003).
[15] B. Andersson, G. Gustafson, and B. Soderbery, Z. Phys. C **20**, 317 (1983).
[16] Z. W. Lin and C. M. Ko, J. Phys. G **30**, S263 (2004).
[17] B. Li, A. T. Sustich, B. Zhang, and C. M. Ko, Int. J. Mod. Phys. E **10**, 267 (2001).
[18] C. M. Ko and L. W. Chen, Nucl. Phys. **A774**, 527 (2006).
[19] J. H. Chen *et al.*, Phys. Rev. C **74**, 064902 (2006).
[20] J. X. Zuo *et al.*, Eur. Phys. J. C **55**, 463 (2008).
[21] B. I. Abelev *et al.* (STAR Collaboration), arXiv:0909.4131 [nucl-ex]; L. Kumar (STAR Collaboration), J. Phys. G **36**, 064066 (2009); J. Y. Chen (STAR Collaboration), arXiv:0910.0556 [nucl-ex].
[22] B. B. Back *et al.* (PHOBOS Collaboration), Phys. Rev. Lett. **97**, 012301 (2006).
[23] R. J. M. Snellings, H. Sorge, S. A. Voloshin, F. Q. Wang, and N. Xu, Phys. Rev. Lett. **84**, 2803 (2000).
[24] H. Liu, S. Panitkin, and N. Xu, Phys. Rev. C **59**, 348 (1999).
[25] J. Brachmann *et al.*, Phys. Rev. C **61**, 024909 (2000); L. P. Csernai and D. Rohrich, Phys. Lett. **B458**, 454 (1999).
[26] L. W. Chen, V. Greco, C. M. Ko, and P. Kolb, Phys. Lett. **B605**, 95 (2005).